on Boundary and Interior Layers
BAIL 2006
G.Lube, G.Rapin (Eds)

Turbulent Boundary Layers: Reality and Myth

Matthias H. Buschmann*
Privatdozent, Institut für Strömungsmechanik, Technische Universität Dresden, Dresden, Germany
Mohamed Gad-el-Hak
Caudill Professor and Chair of Mechanical Engineering,
Virginia Commonwealth University, Richmond, VA 23284-3015, USA

1. Introduction

Hundred years after Ludwig Prandtl's fundamental lecture on boundary layer theory, the mean-velocity profile and the shear-stress distribution of the seemingly simplest case of wall-bounded flow, the zero-pressure-gradient turbulent boundary layer (ZPG TBL), still appears to be *terra incognita*. Even less is known about confined and semi-confined flows undergoing pressure gradients, such as pipe and channel flows and wall-bounded flows approaching pressure-driven separation. The problem is of course related to the lack of analytical solutions to the instantaneous, nonlinear Navier–Stokes equations that govern the stochastic dependent variables of almost all turbulent flows. What little we know about turbulence comes from experiments and heuristic modeling, not first-principles solutions.

One of the fundamental tenets of classical boundary-layer research is the idea that, for a given geometry, any statistical turbulence quantity (mean, rms, Reynolds stress, etc.) measured at different facilities and at different Reynolds numbers will collapse to a single universal profile when non-dimensionalized using the proper length and velocity scales. This is termed self-similarity or self-preservation and allows convenient extrapolation from the low-Reynolds-number laboratory experiments to the much higher-Reynolds-number situations encountered in typical field applications.

During the mid 1990's, a new debate intensified regarding the nature of the mean-velocity profile of canonical turbulent wall-bounded flows. Caused by new unconventional approaches questioning two of the cornerstones of modern fluid mechanics—the logarithmic law of turbulent boundary layers and the independence of its parameters on the Reynolds number, several new scalings were developed. In conjunction with these theoretical investigations, high-quality experiments in zero-pressure-gradient turbulent boundary layers and turbulent pipe and channel flows were undertaken. In general, the physical picture of wall-bounded flow is now much more complex than was thought a decade ago. However, the physical picture seems to be also more controversial than ever before. Which of these new approaches will survive and contribute substantially to fluid mechanics in the future is still open.

In the present paper, we will focus on recent advances in analytical and asymptotic approaches. We will apply a general rule proposed by Fernholz & Finley (1996) in their review paper of ZPG TBL: *In the absence of any complete or convenient theoretical approach, our primary function is to describe what we see.* However, based on these descriptions and physical arguments, we will additionally make judgments with respect to the different approaches discussed here. The discussion will be restricted to steady, incompressible flows over smooth walls that are two-dimensional in the mean. The experimental data sets by Österlund et al. (2000) for ZPG TBL, by McKeon et al. (2004) for fully-developed pipe flows and by Zanoun et al. (2003) for channel flows will be used as benchmarks to validate theoretical ideas. Two standard statistical tools—plotting the theoretical mean velocity values versus the corresponding experimental data and the fractional difference plots—will be employed. Any potential Reynolds number effects will be visualized by coloring the curves representing the mean-velocity profiles according to their individual Reynolds number.

2 Experimental Work and Following Theories

Since the first experimental research on turbulent boundary layers done by L. Prandtl (1904) and his students, the zero-pressure-gradient boundary layer takes a centre stage. To decrypt the functional form of the mean velocity profile and the behavior of the Reynolds shear stress, very often many "real world flow" features are separated out and the so called *canonical turbulent boundary layer* is investigated. The main attributes of such a boundary layer are:

- No pressure gradient in the streamwise direction.
- Incompressible, isothermal, and two-dimensional in the mean.
- Sufficiently high Reynolds number ($Re_{\Theta,\,min} \approx 350–730$) to ensure that the main features of fully developed turbulence occur.
- Neither affected by surface roughness, wall curvature or outer turbulence.
- No upstream disturbances like tripping devices, steps etc.

Other canonical flows are the flow in straight, hydrodynamically smooth circular pipes and rectangular channels with infinitely large aspect-ratio (width/height). However, there is a significant difference between the canonical ZPG TBL on one side and pipe and channel flows on the other side. While the latter are parallel flows, all boundary layers show diverging and in some cases even converging streamlines.

2.1 Zero-pressure-gradient turbulent boundary layer

The analysis of the ZPG TBL data by Österlund et al. (2000) basically confirmed the classical assumption of a Reynolds-number-independent logarithm region. However, this region is found above $y^+ \approx 200$, which contradicts the classical view that the log law region starts at about $y^+ \approx 50-70$. The outer limit of the overlap region was found to be at $y/\delta \approx 0.15$. Following these findings an overlap region with an universal law can therefore exist only above a minimal Reynolds number of $Re_\Theta > 2000$. The parameters found by Österlund et al. (2000) are $\kappa = 0.38$ for the Kármán constant, $B_i = 4.1$ and $B_o = 3.6$ for the additive constants. Differently the low Reynolds number data by Osaka et al. (1998) reveal that κ has a constant value of 0.41, while B_i slightly depends on the Reynolds number but reaches a constant value of about 5.0 for $Re_\Theta > 5.000$. The latter is in agreement—within the bounds of experimental accuracy—with Fernholz & Finley (1996) who found the constants to be 0.40 and 5.1.

Law of the wall: $u^+ = \frac{1}{\kappa} ln\left(y^+ \right) + B_i$; Defect law: $\frac{u_e - u}{u_\tau} = -\frac{1}{\kappa} ln\left(\eta \right) + B_i$ (2.1a, b)

The very brief survey given above might lead to the conclusion that the classical view and recent results of high-Reynolds-number experiments are antagonistic. That this is not necessarily the case was shown by Buschmann & Gad-el-Hak (2003). However, to overcome this seeming discrepancy, a persisting influence of viscosity throughout the entire boundary layer even at very high Reynolds numbers has to be considered. It must be stated in general that the classical logarithmic law is not merely an approximate equation for the mean velocity profile. From the point of view of composite expansion (Panton, 2005), the log law is the limiting behavior of the zeroth-order term of the inner Poincaré series expansion, $f_0\left(y^+ \right)$ as $y^+ \to \infty$, and the limiting behavior of the first-order term of the outer Poincaré series expansion, $F_1\left(\eta \right)$ as $\eta \to 0$. Therefore the parameters of the classical logarithmic law are somewhat circumstantial.

Traditionally, semi-log plots of u^+ versus y^+ are used to compare the inner law with experimental data. This is only useful if the analyzed mean-velocity profiles do not depend on any additional parameters. Therefore, we show herein the profiles according to Equation (2.2a) below. In case the theoretical mean-velocity profiles are in agreement with the experimental data, all points in such a linear-linear plot would collapse on a straight line passing by the origin and having a slope of 45 degree. Additionally, the so-called *fractional difference* (2.2b) is plotted. The smaller the *FD* is, the better the agreement between theory and experiment.

$$ln\left(y^+ \right) = \kappa\left(u^+ - B_i \right); \qquad FD = 100\% \left[ln\left(y^+ \right) - \kappa\left(u^+ - B_i \right) \Big/ ln\left(y^+ \right) \right] \qquad \text{(2.2a, b)}$$

Using the limit established by Österlund et al. (2000), only data above $Re_\Theta > 6000$ are plotted in Figure 2.1. The velocity plot shows a nearly perfect agreement between Österlund's data with the logarithmic law with $\kappa = 0.38$ and $B_i = 4.1$. The agreement is remarkably better than the one obtained with George & Castillo power law (Figure 4.1). Employing classical parameters, $\kappa = 0.41$, $B_i = 5.1$, only for the highest Reynolds numbers, a satisfactory agreement is obtained. Of course the quality of both laws is different in different regions of the profile. Comparing only the profiles having the highest Reynolds numbers the *FD* plots show that lower border of Österlund's logarithmic law almost joins the upper border of the classical log law region.

2.2 Pipe flow

In the following we will concentrate on the so-called *superpipe* experiments recently conducted at Princeton University (McKeon et al., 2004). The superpipe is a closed-loop air facility, and the whole system is pressurized to obtain Reynolds numbers up to 36 millions built with pipe diameter (12.9 cm) and bulk velocity.

Analyzing the superpipe data, McKeon et al. (2004) discovered that two regions are distinguished, one following a power law and another following a logarithmic law. The log law having the constant parameters of $\kappa = 0.421 \pm 0.002$ and $B_i = 5.60 \pm 0.08$ is observed in the superpipe data for Reynolds numbers larger than about 2.3×10^4. The range of wall-normal coordinate covered is $600 < y^+ < 0.12\,\delta^+$. The power law region exists close to the wall ($50 < y^+ < 300$). Both the multiplicative factor and the exponent are Reynolds number independent. Their values are very close to the numbers known from Nikuradse's (1932) $1/7^{th}$-power law. Any power law with positive sign changes the straight line known from the usual semi-logarithmic plot to a concave shape. To meet the profile of the viscous sublayer, the profile therefore has to form a "bump" below the power law region. The existence of such a bump in ZPG TBL was shown by Buschmann & Gad-el-Hak (2003).

Despite McKeon's power law is Reynolds number independent we use the plots described for for Barenblatt's Reynolds-number-dependent power law (3.7, 8).

2.3 Channel flow

High-quality channel flow data covering a wide range of Reynolds number are rare. One of the few data sets available was taken by Zanoun et al. (2003) in air using single hot-wire probe. The channel had an aspect ration (width:height) of 12:1 (600×50 mm^2). The wall skin-friction was determined independently of any assumptions concerning the mean flow profile. The research team employed oil film interferometry, and the Reynolds number range was $5.33 \times 10^4 \le Re_H \le 2.27 \times 10^5$. The major finding of Zanoun's work is the confirmation of the classical logarithmic law, in straight channels. The parameters are again different, however $\left(\kappa \approx 1/e = 0.368..., \; B_i \approx 10/e = 3.678... \right)$.

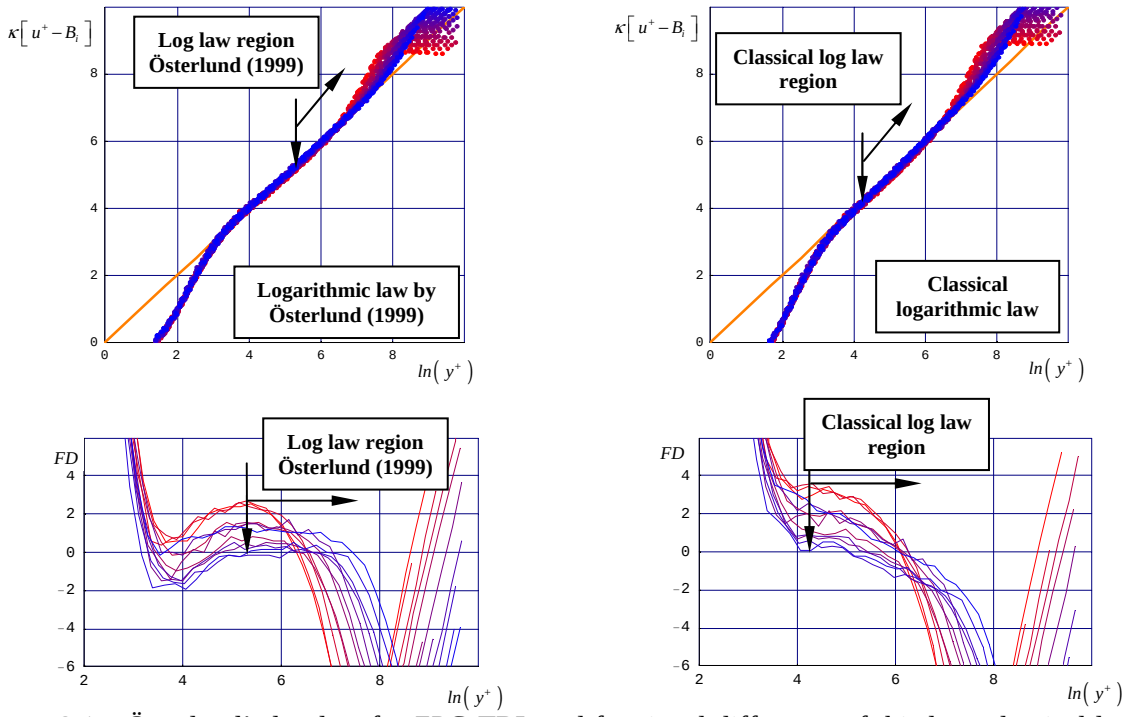

Figure 2.1 Österlund's log law for ZPG TBL and fractional difference of this law, classical log law and fractional difference of this law. ZPG TBL data from Österlund et al. (2000).

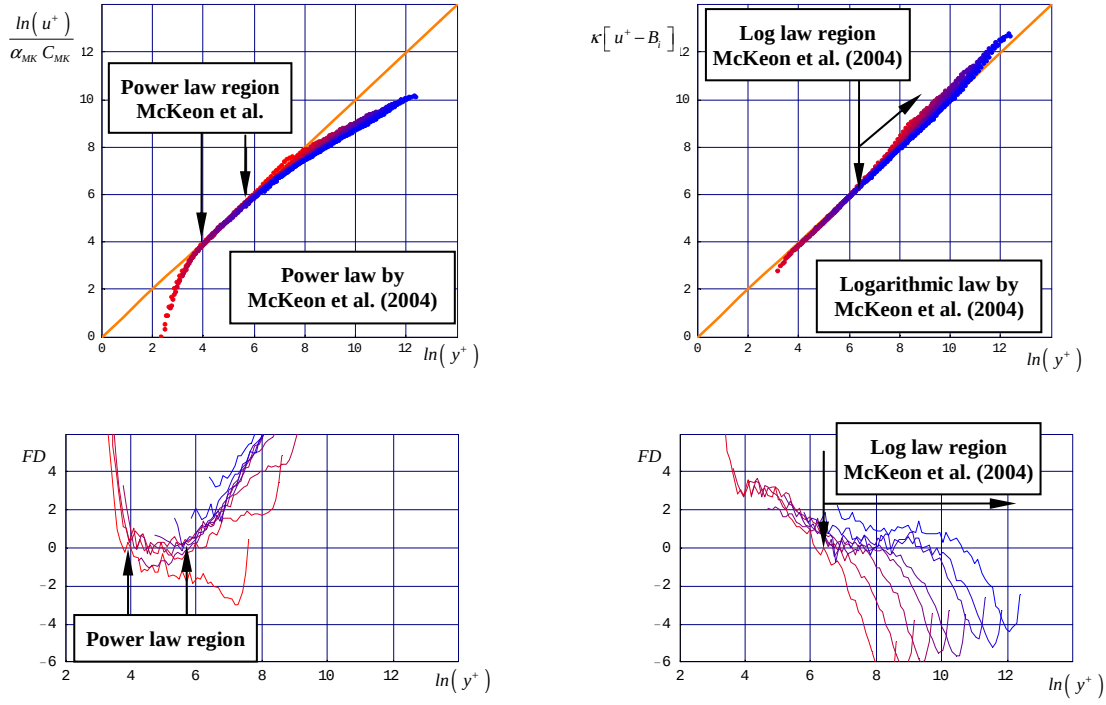

Figure 2.2 McKeon's power law and fractional difference. McKeon's log law and fractional difference. Pipe flow data by McKeon et al. (2004).

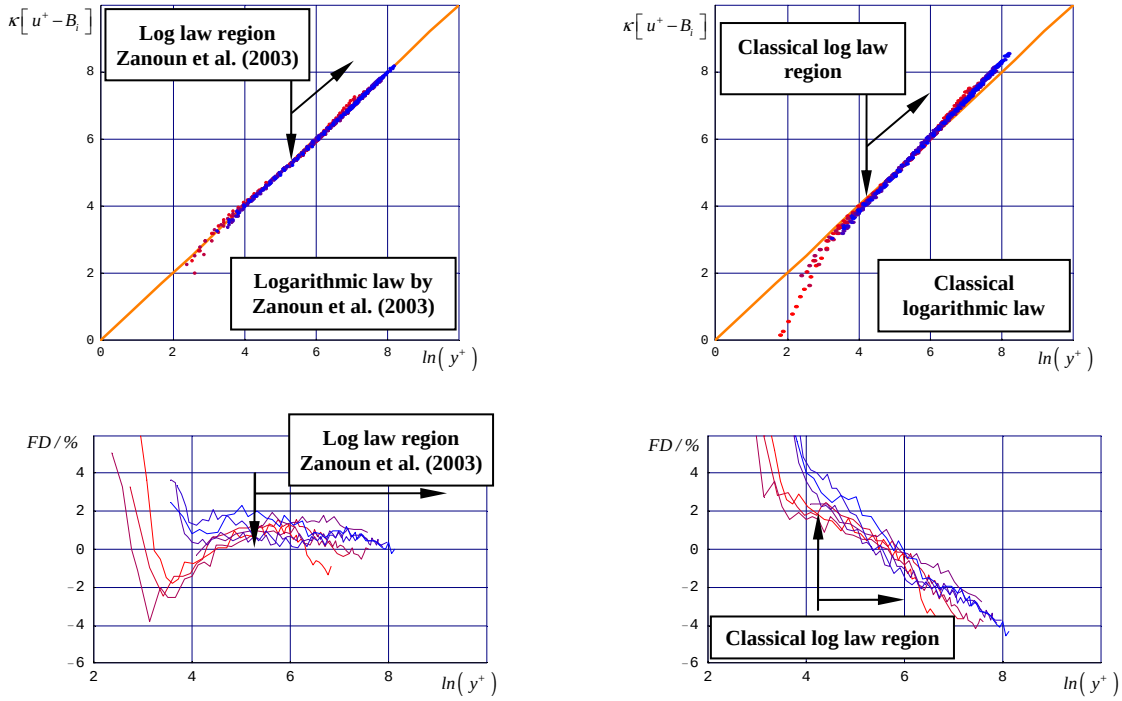

Figure 2.3 Zanoun's log law for ZPG TBL and fractional difference of this law, classical log law and fractional difference of this law. Channel flow data are from Zanoun et al. (2003).

3. Power Law by G. I. Barenblatt

In a series of papers G. I. Barenblatt, A. J. Chorin and V. M. Prostokishin developed, based on principle of intermediate asymptotic, a power-law-type scaling law for the mean velocity profile of zero-pressure gradient TBL and pipe flow. One of the fundamental ideas of this group is the distinction between *complete* and *incomplete similarity*.

Outgoing from the finding that the Kármán constant of Millikan's logarithmic law (Millikan, 1938), reveals a systematic dependence on the Reynolds number Barenblatt (2003) postulates two hypotheses:

First hypothesis — *There is an incomplete similarity of the mean velocity gradient in the parameter $y^+ = u\,y\,/\,\nu$ and no kind of similarity in the Reynolds number.*

Second hypothesis — *The gradient of average velocity tends to a well-defined limit as the viscosity vanishes.*

According to the first hypothesis, the influence of the viscosity remains at arbitrary large Reynolds numbers in the entire boundary layer, not just in the viscous sublayer.

The gradient of the mean-velocity profile is adopted as starting point for the derivation of the functional form of the profile. It is assumed that the governing parameters are τ_w, ρ and y, their

dimensions are independent. Introducing the local friction velocity u_τ the following similarity numbers are obtained

$$y^+ = u_\tau\, y / \nu\,; \qquad \text{and} \qquad Re_\Lambda = \Lambda\, u_\tau / \nu \tag{3.1a, b}$$

While y^+ is a local Reynolds number with respect to the wall-normal coordinate, Re_Λ is the global Reynolds number. Rewriting (3.1b) it becomes obvious that the latter is actually the ratio of outer and inner length scales. Barenblatt and co-workers assume incomplete similarity and get

$$\frac{y}{u_\tau}\frac{\partial u}{\partial y} = y^+ \frac{\partial u^+}{\partial y^+} = g\left(Re_\Lambda\right) \times y^{+\alpha} \qquad \text{with} \qquad \alpha = \alpha\left(Re_\Lambda\right) \tag{3.2}$$

The strong assumption here is that the functional form of (3.2) behaves as a power law. Integrating under the assumption that the integration constant is zero, Barenblatt's power law is obtained. The remaining parameters were found by Barenblatt & Prostokishin (2003) by analyzing the classical pipe flow data-base of Nikuradse (1932).

$$u^+ = C\left(Re_\Lambda\right) y^{+\alpha}; \qquad \alpha = \frac{3}{2\, ln\left(Re\right)}; \qquad C = \frac{1}{\sqrt{3}}\, ln\left(Re\right) + \frac{5}{2} = \frac{\sqrt{3} + 5\alpha}{2\alpha} \tag{3.3a, b, c}$$

3.2 Experimental evidence of Barenblatt's power law

Plotting experimental data according to (3.5, 6) using the usual "+" variables leads to a band of curves. Due to the inherent Reynolds number dependence, no collapse of the data can be achieved. Equation (4.5) has therefore to be reformulated to obtain a universal relation (3.4a). Additionally, the fractional difference of (3.3a) is plotted in the bottom portion of Figure 3.1,

$$ln\left(y^+\right) = \frac{1}{\alpha}\, ln\left(\frac{u^+}{C}\right); \qquad FD = 100\% \left[ln\left(y^+\right) - \frac{1}{\alpha}\, ln\left(\frac{u^+}{C}\right)\right] \Big/ ln\left(y^+\right) \tag{3.4a, b}$$

Using the super-pipe data by McKeon et al. (2004), we plot in Figure 3.1 Barenblatt's power law. The figures reveal the following:

I. For high Reynolds numbers there might be a power law region that can be seen as plateau in the lower left diagram. But this plateau shows a Reynolds number dependent albeit constant departure from a zero fractional difference.
II. The smaller the Reynolds number becomes, the smaller the plateau becomes. For the smallest Reynolds number involved, the plateau disappears completely and is displaced by a steep line.

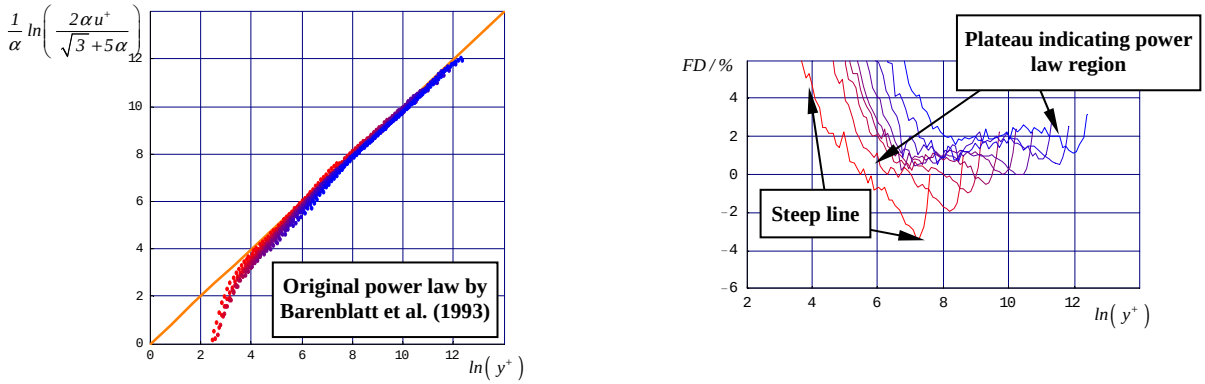

Figure 3.1 Barenblatt's power law and fractional difference. Pipe flow data by McKeon et al. (2004).

4. The Approach by W. K. George and Colleagues

The school lead by W. K. George developed a power law that is derived from the Prandtl's boundary layer equation (George & Castillo 1997; Castillo & George, 2001). Their approach is quite different from that of Barenblatt and colleagues whose power law stems from dimensional analysis. Unlike Barenblatt's power law, however, George's power law is valid only for ZPG TBL.

The approach by George and co-workers is associated with three key concepts:

I. Search for similarity separately for the inner and the outer layer

Consider the complete boundary layer equation for incompressible, two-dimensional steady flow. Arguing that "*the no-slip condition precludes the possibility of similarity solutions for the entire boundary layer*" (George & Castillo, 1997), similarity solutions are sought that accomplish asymptotically for infinite Reynolds number the degenerated momentum equations for inner region and the outer region separately.

II. Asymptotic Invariance Principle

The Asymptotic Invariance Principle (AIP) proposed by George (1995) is based on three lemmata:

Lemma 1 The full mean momentum equation has Reynolds number dependent terms that disappear only for $Re \to \infty$. Any similarity solution of this equation for finite Reynolds numbers will therefore be Reynolds number dependent.

Lemma 2 The degenerated mean momentum equations for the inner and the outer regions are only exactly valid for $Re \to \infty$. Any similarity solutions of these equations will therefore be exactly valid only in this limit.

Lemma 3 Similarity solutions found for the degenerated mean momentum equations have the same functional shape as the sought scaling laws for finite Reynolds number.

According to Lemma 1, the sought solutions must always be Reynolds number dependent. According to Lemma 3, their functional shape can be determined by employing degenerated inner and outer representation of mean momentum equation.

III. Near Asymptotic

Having obtained the scaling by employing AIP, a next step has to be undertaken to find the functional forms of the mean velocity profile in the common region. This is done by assuming that inner and the outer velocity profile degenerate at infinite Reynolds number in different ways. For detailed derivation, see George & Castillo (1997). For ZPG TBL the following profiles are obtained.

$$u^+ = C_i\left(\delta^+\right)\left(y^+ + a^+\right)^{\gamma\left(\delta^+\right)}; \qquad u/u_e = C_o\left(\delta^+\right)\left(\overline{y} + \overline{a}\right)^{\gamma\left(\delta^+\right)} \tag{4.1, 2}$$

The finding of a power law is not surprising because two different velocity scales are employed in the inner region and the outer region. The offset a^+ was originally introduced to make (4.1, 2) invariant to coordinate transformation of the form $y \to y + a$ (George & Castillo, 1997). Later this parameter was interpreted as an influence coming from the so-called mesolayer. Such a layer is understood as a region where neither dissipation nor Reynolds stress will become independent of viscosity no matter how high the Reynolds number is.

One of the consequences of the AIP is that, differently to the classical view based on Millikan's assumptions for $Re \to \infty$, the shape parameter, δ_* / θ lingers larger than unity and the skin-friction coefficient c_f remains larger than zero. This is indeed surprising because the shape parameter compares the boundary layer flow with the potential flow and the skin-friction coefficient stands for the no-slip condition occurring only in flows affected by molecular viscosity. The Millikan's

assumptions $(\delta_* / \theta)\big|_{Re\to\infty} \to 1$ and $c_f\big|_{Re\to\infty} \to 0$ basically say *no viscosity, no boundary layer and no boundary-layer effects*, which is in agreement with Prandtl's ideas regarding wall-bounded flows.

Based on AIP and near asymptotic, Wosnik et al. (2000) found a logarithmic law for pipe and channel flows. Whilst fully-developed pipe and channel flows are always parallel flows, any TBL exhibits divergence or convergence of the mean streamlines. Pipe and channel flow are therefore characterized by only one velocity scale namely u_τ, which leads following AIP to a logarithmic law

$$u^+ = \frac{1}{\kappa\left(\delta^+\right)} ln\left(y^+ + a^+\right) + B_i\left(\delta^+\right); \qquad \frac{u - u_{cl}}{u_\tau} = \frac{1}{\kappa\left(\delta^+\right)} ln\left(\bar{y} + a\right) + B_o\left(\delta^+\right) \qquad (4.3, 4)$$

4.1 Experimental evidence of the George–Castillo power law

For testing George-Castillo power law Österlund's ZPG TBL data are employed. Wosnik's logarithmic law (4.3) is tested using the super-pipe data by McKeon et al. (2004). For plotting the data, we either apply (3.4a, b) or (2.2a, b). The power-law parameters are calculated according to George & Castillo (1997) and the log-law parameters are taken from Wosnik et al. (2000).
Figure 4.1 shows that employing the George–Castillo power law most of Österlund's data collapse in a straight line. However, this line does not coincide with the diagonal of the diagram. This indicates a power law region may exist but with different parameters. Let's compare the George–Castillo power law with the one found by Nikuradse (1932) for pipe flow but very often employed for TBL. For simplicity the parameters are set constant and chosen 1/7 (power) and 8.42 (coefficient). Again the majority of Österlund's data collapse in a straight line and an almost parallel bunch of curves is obtained in the fractional difference. Another time the idea that the mean velocity profile of a ZPG TBL might be at least partly described by a power law is supported. One of the major differences between the classical log law and the one proposed by Wosnik is immediately visible from Figure 4.2. Due to the internal additive constant, the data in the buffer layer are forced to collapse with the diagonal. Further out, there seems to be a region of good agreement between predicted and experimental values.

5. Higher order approaches

So far we have seen that recent approaches concerning the velocity profile of turbulent wall-bounded flow do neither rule out log nor power law behaviour. Additionally, a Reynolds number dependency of the mean-velocity profile cannot be excluded in general. From that the straightforward conclusion follows that a much more complex functional form is needed to describe the profile.

The recent higher order approach by Buschmann & Gad-el-Hak (2003) is based on the assumption that at sufficiently high Reynolds number the influence of the outer turbulence-structures scaling with δ diminishes on the inner zone, and the influence of the inner viscosity dominated structures scaling with ν / u_τ diminishes on the outer zone. The interaction between both zones decreases as well, but never disappears totally and Reynolds-number effects will persist also for high Reynolds numbers. Based on that fundament two major hypotheses are employed by Buschmann & Gad-el-Hak (2003):

1. The classical two layer assumption is sufficient to describe a wall-bounded flow.
2. Asymptotic matching can be applied to obtain higher order solutions for the mean velocity profile in the overlap region.

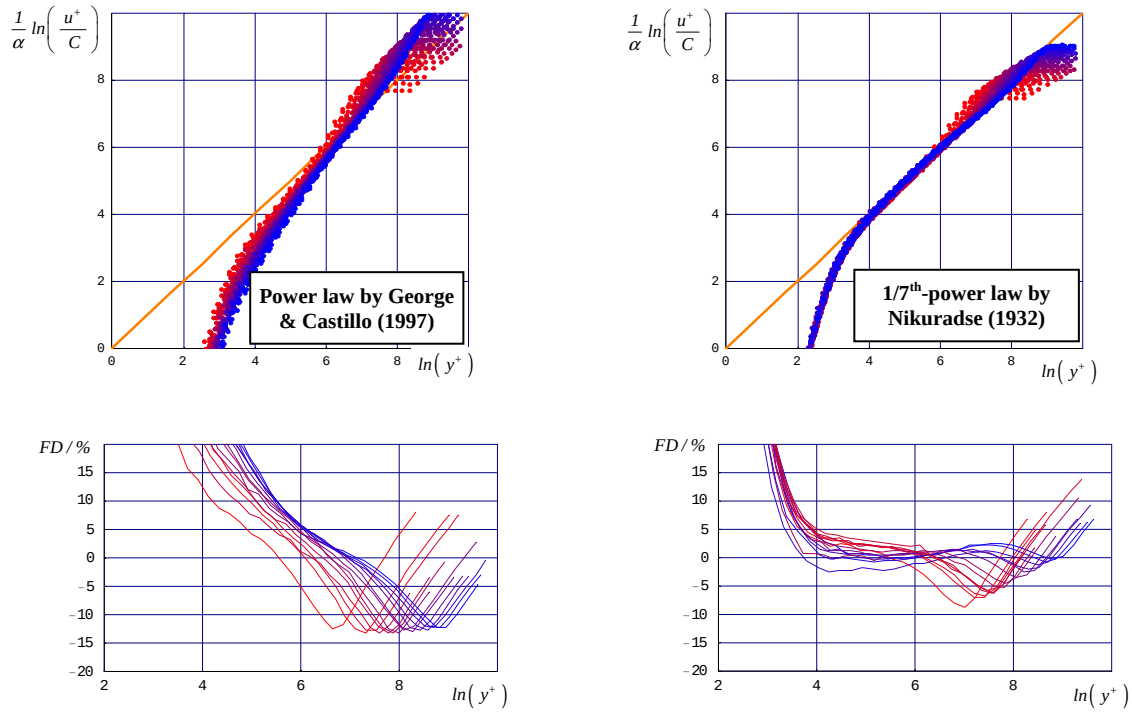

Figure 4.1 The George–Castillo power law for ZPG TBL and fractional difference of this law. Nikuradse's 1/7th-power. ZPG TBL data from Österlund et al. (2000).

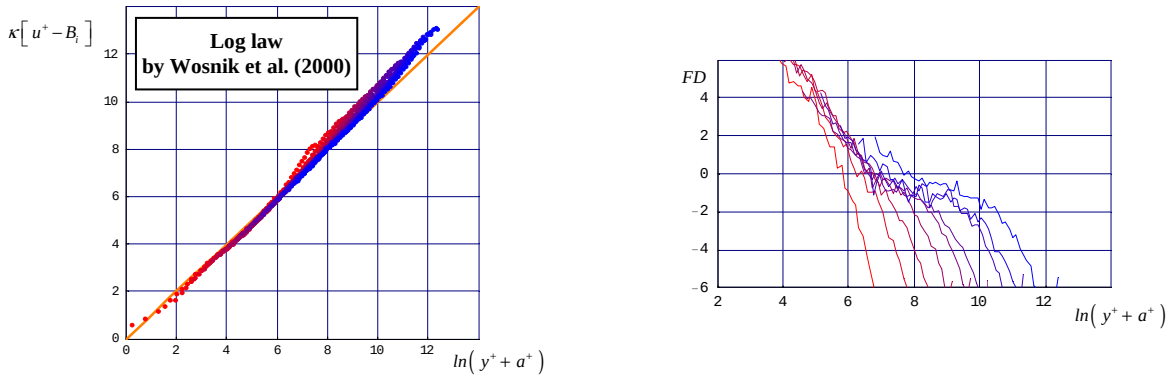

Figure 4.2 Wosnik's log law for pipe flow and fractional difference of this law. Pipe flow data from McKeon et al. (2004).

Asymptotic expansions are formulated for inner and outer region separately

$$u^+ \sim \sum_{i=0}^{\infty} u_0^+\left(y^+\right)\gamma_0\left(\delta^+\right); \qquad U \sim \sum_{i=0}^{\infty} U_0\left(\eta\right)\Gamma_0\left(\delta^+\right) \tag{5.1a, b}$$

Here γ_i and Γ_i represent gauge functions which depend only on δ^+ but do not necessarily have the same functional shape. In general the strong assumption is here the separation of the Reynolds-number dependence and the dependence on the wall-normal coordinate into multiplicative functions. Because turbulence is not a closed problem, the selection of the gauge functions always needs additional

assumptions. Preferably these assumptions are founded on first principles. Afzal (1976) introduced based on a consideration of the governing equation of the mean momentum of pipe and channel flow.

$$\gamma_i = \Gamma_i = 1 / \delta^{+\,i} \tag{5.2}$$

Matching (5.1a) and (5.1b) properly leads to the generalized logarithmic law for the inner region

$$u^+ = \underline{\frac{1}{\kappa_0} ln\left(y^+ \right) + C_0 + \sum_{j=1}^{\infty} \frac{E_{0,j}}{y^{+\,j}}} + \sum_{i=1}^{\infty} \varepsilon^i \left[\frac{1}{\kappa_i} ln\left(y^+ \right) + C_i + \sum_{j=1}^{i} B_{i,j}\, y^{+\,j} + \sum_{j=1}^{\infty} \frac{E_{i,j}}{y^{+\,j}} \right] \tag{5.3}$$

and an equivalent generalized defect law. The parameters $1/\kappa_i, C_i, B_{i,j}, E_{i,j}, c_i, b_{i,j}$ and $e_{i,j}$ must be determined from experimental data. Equation (5.3) clearly indicates that pure logarithmic regions do not exist at least not in pipe and channel flow. The nonlogarithmic, higher-order terms of y^+ and δ^+ persist throughout the entire overlap region and for all finite Reynolds numbers. Beside the constant and the logarithmic terms two types of nonlogarithmic terms are found with (5.3). The first group consists of terms becoming strong close to the wall and have functional forms of $E_{i,j} / y^{+\,j}$. These terms allow extending the classical logarithmic law into the upper regions of the buffer-layer. The second new group of terms consist of terms becoming strong in the inner wake zone. For the inner generalized log law these terms have the shape of $B_{i,j}\, y^{+\,j}$. All higher order terms mentioned above disappear for $Re \to \infty$ and the classical log law (3.1a) remains.

5.1 Experimental evidence of the generalized logarithmic law

The generalized log law (5.3) contains an infinite number of constants. Currently it is not known if this manifold can be reduced to more complex functions. Therefore the law has to be truncated carefully. Here results of a second order solution are presented.

The successful application of the generalized log law for ZPG TBL was shown by Buschmann & Gad-el-Hak (2003). In here using the super-pipe data by McKeon et al. (2004) the superior application to pipe flow is shown (Figure 5.1). One may argue that any higher-order solutions is condemned to success because of the larger number of free parameters involved (Panton, 2005). But this is only partly true because a higher-order solution as the generalized law based on first principles and adopting only a minimum of assumptions bears essentially more physics in it than a simple approach.

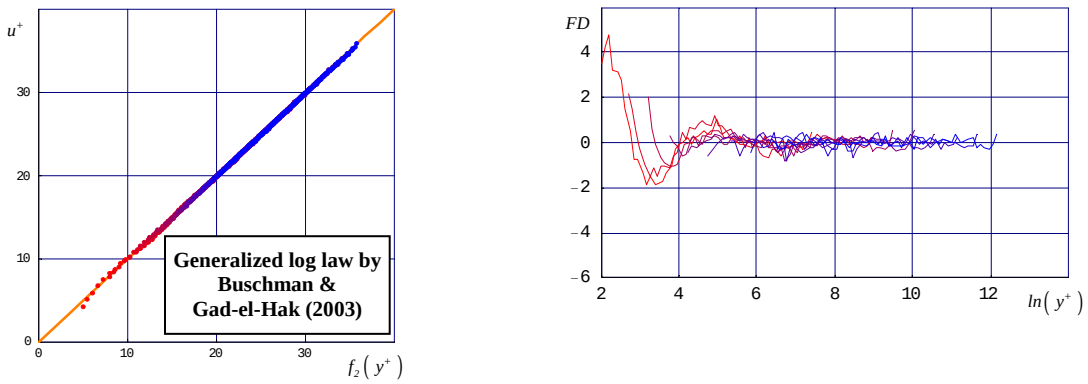

Figure 5.1 Buschmann & Gad-el-Hak's second order generalized log law and fractional difference. Pipe flow data are from McKeon et al. (2004).

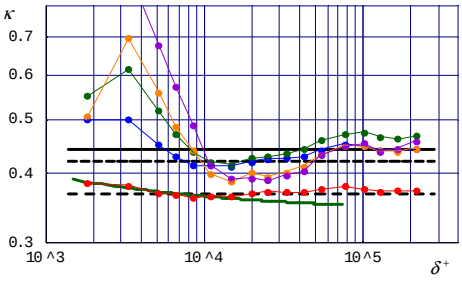

Figure 5.2 Kármán constant depending on the order of the generalized logarithmic law
Red: n = 0, blue: n = 1, green: n = 2, orange: n = 3 and violet: n = 4.
— Tennekes (1968), – – $\kappa = 0.368$ Zanoun et al. (2003),
····· $\kappa = 0.421$ McKeon et al. (2004),
— $\kappa_\infty = 0.447$ Wosnik et al. (2000)

Collecting terms of identical functional form (logarithmic, constant etc.) reveals that the well-known parameters of the classical log law become Reynolds-number dependent functions. An example is the Kármán constant.

$$\frac{1}{\kappa} = \sum_{i=0}^{\infty} \frac{1}{\delta^{+i}} \frac{1}{\kappa_i} \tag{5.4}$$

Figure 5.2 compiles the Reynolds-number dependence of (5.4) up to fourth order of (5.3). It has to be emphasized that this parameter is only valid for pipe flow because (5.3) covers parts of the usual wake region which is different for ZPG TBL, channel and pipe flow. Interestingly enough for medium Reynolds numbers the parameters calculated with the zeroth-order solution are very close to the values proposed by Zanoun et al. (2003) for channel flow. However, the Kármán constant shows a slight Reynolds number which is in excellent agreement with a function for κ given by Tennekes in 1968

$$\kappa_{TN} = 2.95 - 4.40 \,/\, \delta^{+1/3} \tag{5.5}$$

Remarkably Tennekes function has a similar form as (5.4) except the power is not integer. The agreement can be explained by the similarity of the law investigated by Tennekes (pure logarithmic law) and the zeroth-order solution (underlined terms of (5.3)). The value of this finding is clear. Long before the recent debate the Reynolds number dependency of the mean velocity profiles of pipe was discovered, using a database which was completely independent of nowadays pipe flow data.
The higher order solutions show that both parameters asymptote nonmonotonically to values which are very similar to the high Reynolds number parameters given by Wosnik et al. (2000) for turbulent pipe and channel flow. The coincidence of both results is explainable by the facts that first both theories are based on the two-layer assumption and asymptotic matching is employed to obtain the mean velocity profile in the overlap region, second both theories demand the inclusion of finite Reynolds number effects and third both approaches lead for $Re \to \infty$ to pure logarithmic functions. The major differences between the generalized log law and the law by Wosnik et al. (2000) are the functional shape of the mean velocity profile at finite Reynolds numbers and the functional dependence of the parameters like κ on the Reynolds number.

To summarize the higher order approach proposed by Buschmann & Gad-el-Hak (2003) show excellent agreement with experimental pipe flow and ZPG TBL data. Together with other higher order approaches it clearly demonstrates that involving both higher order Reynolds-number effects *and* higher order effects of the dependency on the wall-normal coordinate is advantageous. However, to be successfully such an approach must be based on first principles and has to employ only a minimum of additional physical assumptions.

6. Summary

In closing we summarize that in the last decade a new debate on the general behavior of wall-bounded flows started. The majority of the attempts can be categorized as either:

I. deriving the shape and the corresponding parameters of the mean velocity profile directly from high quality experimental data or

II. employing theoretical considerations with the same task.

Some of the later are based on first principle, some apply asymptotical approaches others are founded on dimensional analysis only. However, none of them is directly based on the modelling of turbulent motion. Keeping in mind that the task of all approaches discussed above is to find the time averaged representation of a *turbulent motion* this seems to be a general deficit. This is especially true for any theory which is not based on first principles and takes instead more or less gratuitous assumptions into account. Unfortunately, due to the closing problem of turbulence, incorporating physical assumptions cannot be avoided completely.

Employing the probably best data sets currently available world wide we have uncover the qualities of several approaches. However, this still says nothing about the general physical correctness of a certain approach. We therefore accompanied our investigation with a discussion of the physical features of these approaches. The outcome can be summarized with the following statement: The mean velocity profile of turbulent wall-bounded flows is much more complex than the classical log law or a simple power law. A Reynolds number dependence of the mean profile persisting for arbitrarily high but finite Reynolds numbers seems to be highly likely. At least this dependence if not the whole profile seems to be different for boundary layers on one side and confined flow (pipe, channel) on the other side. Both experimental and theoretical work is needed to resolve these questions.

References

[1] H.H. Fernholz, P.J. Finley, "The incompressible zero-pressure-gradient turbulent boundary layer: An assessment of the data", *Prog. Aerospace Sci.*, **32**, 245–311 (1996).

[2] J.M. Österlund, A.V. Johansson. H.M. Nagib, M.H. Hites, "A note on the overlap region in turbulent boundary layers", *Physics of Fluids*, **12**, 1–4 (2000).

[3] B.J. McKeon, J. Li, W. Jiang, J.F. Morrison, A.J. Smits, "Further observations on the mean velocity distribution in fully developed pipe flow", *J. Fluid Mech.*, **501**, pp. 135–147, (2004).

[4] E.-S. Zanoun, F. Durst, H.M. Nagib, "Evaluating the law of the wall in two-dimensional fully developed turbulent channel flows", *Physics of Fluids*, **15**, 3079–3089, (2003).

[5] L. Prandtl, "Über Flüssigkeitsbewegung bei sehr kleiner Reibung", In: Verhandlungen des dritten internationalen Math. Kongresses, Heidelberg, Teubner Verlag, Leipzig, 484–491, (1904).

[6] H. Osaka, T. Kameda, S. Mochizuki, "Re-examination of the Reynolds number effect on the mean flow quantities in a smooth wall turbulent boundary layer", *JSME International Journal*, **41**, 123–129, (1998).

[7] M.H. Buschmann, M. Gad-el-Hak, "Generalized logarithmic law and its consequences", *AIAA-Journal*, **41**, 40–48, (2003).

[8] R.L. Panton, "Review of wall turbulence as described by composite expansions", *Appl. Mech. Rev.*, **58**, 1–36, (2005).

[9] J. Nikuradse, "Gesetzmäßigkeiten der turbulenten Strömung in glatten Rohren", *VDI-Fortschritt-Heft*, no. 356, (1932).

[10] C.B., Millikan, "A critical discussion of turbulent flows in channels and circular tubes", *Proceedings of the Fifth International Congress on Applied Mechanics*, eds. J. P. Den Hartog and H. Peters, Wiley, New York, 386–392 (1938).

[11] G.I. Barenblatt "Scaling laws for fully developed turbulent shear flows. Part 1: Basic hypotheses and analysis", *J. Fluid Mech.*, **248**, 521–529, (1993).

[12] G.I. Barenblatt, V.M. Prostokishin, "Scaling laws for fully developed turbulent shear flows. Part 2: Processing of experimental data", *J. Fluid Mech.*, **248**, 513–520 (1993).

[13] W.K. George, L. Castillo, "Zero-Pressure-Gradient turbulent boundary layer", *Applied Mech. Rev.*, **50**, 689–729 (1997).

[14] L. Castillo, W.K. George, "Similarity analysis for turbulent boundary layer with pressure gradient: Outer flow", *AIAA-Journal*, **39**, 41–47 (2001).

[15] M. Wosnik, L. Castillo, W.K. George, "A theory for turbulent pipe and channel flows", *J. Fluid Mech.*, **421**, 115–145 (2000).